Circulation Generation and Vortex Ring Formation by Conic Nozzles

Moshe Rosenfeld
School of Mechanical Engineering,
Tel Aviv University,
Tel Aviv 69978, Israel

Kakani Katija

John O. Dabiri

Graduate Aeronautical Laboratories and
Bioengineering,
California Institute of Technology,
Pasadena, CA 91125

Vortex rings are one of the fundamental flow structures in nature. In this paper, the generation of circulation and vortex rings by a vortex generator with a static converging conic nozzle exit is studied numerically. Conic nozzles can manipulate circulation and other flow invariants by accelerating the flow, increasing the Reynolds number, and by establishing a two-dimensional flow at the exit. The increase in the circulation efflux is accompanied by an increase in the vortex circulation. A novel normalization method is suggested to differentiate between two contributions to the circulation generation: a one-dimensional slug-type flow contribution and an inherently two-dimensional flow contribution. The one-dimensional contribution to the circulation increases with the square of the centerline exit velocity, while the two-dimensional contribution increases linearly with the decrease in the exit diameter. The two-dimensional flow contribution to the circulation production is not limited to the impulsive initiation of the flow only (as in straight tube vortex generators), but it persists during the entire ejection. The two-dimensional contribution can reach as much as 44% of the total circulation (in the case of an orifice). The present study offers evidences on the importance of the vortex generator geometry, and in particular, the exit configuration on the emerging flow, circulation generation, and vortex ring formation. It is shown that both total and vortex ring circulations can be controlled to some extent by the shape of the exit nozzle.
[DOI: 10.1115/1.3203207]

Keywords: vortex ring, circulation, nozzle, laminar flow, CFD

1 Introduction

The present paper studies the generation of circulation and vortex rings using conic converging static nozzles in an attempt to control or manipulate the emerging flow field. The kinematics and dynamics of vortices formed by starting the flow through parallel-walled tubes were studied extensively in experiments over the past 70 years [1–8]. Theories and numerical simulations were implemented to reproduce many of the salient features of the vortex formation process, such as initial vortex sheet rollup [9] and vortex pinch-off [10–14].

A common way of generating vortex rings is by pushing a piston in a tube [1,3–5]. Two main vortex generator configurations have been considered: either a tube with an exit protruding into the flow field, referred to as a *nozzle*, or a tube with an exit flushed with a vertical plate, referred to as an *orifice*. Rosenfeld et al. [10] did not observe significant differences in the maximal total circulation between the two configurations ($<2\%$), but the formation number (see definition in Gharib et al. [5]) was slightly lower for the orifice (3.83 versus 3.97) due to vorticity cancellation of the forming vortex with the side walls. Gharib et al. [5] found experimentally larger differences in the formation number (3.6 and 4.2 for the orifice and nozzle cases, respectively). Mohseni et al. [13] generated numerically vortex rings by applying a nonconservative force rather than conventional piston/tube arrangements. Nevertheless, the properties of the formed vortex rings were similar to those generated by a piston in a tube, and they were also affected by the generation characteristics, such as the amplitude and duration of the forcing.

In addition to these vortex generator types, one can envision employing nozzles with an axially varying cross section to decrease the exit area, and thus, to control the exit flow conditions, such as the mean velocity and the velocity profile. Such exit configurations can be found in numerous biological systems. Intracardiac blood flow and aquatic propulsion are two areas of active research in which the dynamics of the starting flow through conic-like nozzle geometries is known to govern the overall system performance [15,16]. The shape of the vortex generator, and in particular, the exit geometry, may have a significant influence on the vortex ring formation and pinch-off since the rate of generation of the motion invariants (circulation, impulse, and kinetic energy) depend on the details of the flow in the vortex generator. Indeed, Allen and Naitoh [17] and Dabiri and Gharib [18] manipulated the circulation production rate, vortex circulation, and energy by dynamically closing an orifice or opening/closing a nozzle, respectively.

The most widely used analytical tool for predicting the formation kinematics of vortex rings employing parallel wall vortex generators is the slug model approximation for the vorticity flux generated by the starting flow [1,4]. By assuming the vorticity in the flow to be confined into a very thin layer near the wall, one can derive a simple expression relating the circulation flux to the spatially averaged axial velocity U_e of the jet efflux $d\Gamma/dt(t) = (1/2)U_e^2(t)$, where t is the time, and Γ is the accumulated circulation. The slug model has had reasonable success in matching theoretical predictions with empirical measurements of vortex formation from parallel-walled tubes, as long as the discharge duration is short, and the Reynolds number is large [4]. However, its prominent role in current modeling efforts is more closely related to its ease of use rather than accuracy.

The case of the starting flow through conic nozzle geometries is inherently beyond the purview of the slug model, due to the existence of nonzero transverse velocity components in the ejected jet, resulting from the two-dimensional nature of the flow at the exit. These components are also present during the early stages of vortex formation from parallel-walled tubes [1,19]. However, in the latter case, their contribution represents a nearly constant shift in the circulation production, and thus, can be resolved by the addition of an empirical constant. By contrast, in conic nozzle

Contributed by the Fluids Engineering Division of ASME for publication in the JOURNAL OF FLUIDS ENGINEERING. Manuscript received April 14, 2009; final manuscript received July 8, 2009; published online August 18, 2009. Assoc. Editor: Mark Stremler.

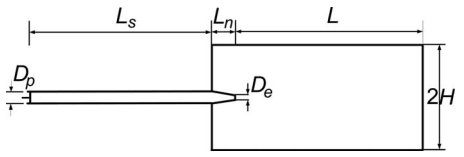

Fig. 1 Sketch of the domain of computation

geometries, the relationship between the vorticity flux and the transverse velocity component is nonlinear and time dependent.

The present study is limited to vortex generators employing static rigid and conic nozzles. The goal is to study circulation generation and vortex ring formation for this simple, yet unexplored geometry, as a starting point for the full comprehension of the dynamically varying nozzles. The present Navier–Stokes numerical simulations demonstrate the ability to control and manipulate the emerging flow.

2 Methods

2.1 Numerical Model. A sketch of the axisymmetric computational domain is given in Fig. 1. The vortex generator has two sections: a straight tube of length $L_s=40$ cm and a constant diameter of $D_p=2.5$ cm, and a conic nozzle of length $L_n=5.1$ cm (the dimensions are chosen to match the experimental setup) and exit diameter D_e of $D_e/D_p=0.2$, 0.4, 0.6, 0.8, or 1. The computational domain downstream of the nozzle exit has a length of $L/D_p=32$, and the outer boundary is at a radial distance of $H/D_p=4$. Numerical experiments have verified that the downstream and outer boundaries are placed far enough from the region of interest.

The moving piston is modeled as a uniform velocity inlet. Undocumented simulations performed in the course of the present study proved that this model produces results that are very similar to a moving piston, as long as the maximal stroke length is smaller than the length of the vortex generator. An impulsive velocity program of the piston is used with a constant piston velocity of $U_p=2$ cm/s in all the cases of the present study. Two velocity programs are used: (i) a continuous inflow velocity (velocity program no. 1) and (ii) the constant inflow is stopped at a given dimensionless time (velocity program no. 2). On the outer and downstream boundaries, zero gauge pressure is specified. On all the other boundaries, wall conditions are given, except on the axis of symmetry.

The axisymmetric, incompressible, time dependent, and laminar Navier–Stokes equations have been solved using the finite-volume package of FLUENT 6.23, ANSYS, Inc. Second-order accurate temporal and spatial schemes have been used with pressure-implicit with splitting of operators (PISO) pressure-velocity coupling. Mesh-size and time-step independence tests have been performed, resulting in a mesh of 180,000 nodes with clustering in the shear layer and near the walls, and a maximal dimensionless time step of $\Delta t_e^*=(U_e\Delta t/D_e)0.02$, where Δt is the uniform time step. The difference in the circulation of the selected mesh relative to a finer mesh with 685,000 nodes is less than 1%, and relative to a time step, twice as fine, is less than 0.1%.

2.2 Dimensionless Parameters. The choice of nondimensional parameters is not obvious in the present case since two velocity scales exist—one is the piston velocity (that remains constant in all the cases) and the other is the spatial average exit velocity U_e (that depends on the diameter of the nozzle exit). The corresponding length scales are the piston diameter and the nozzle-exit diameter, respectively. Gharib et al. [5] suggested for a straight tube vortex generator a dimensionless formation time defined by

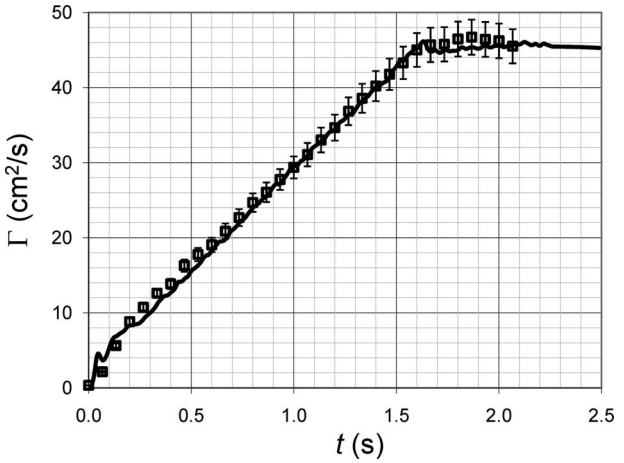

Fig. 2 Comparison of the circulation evolution of the numerical (solid line) and experimental (symbols) results ($D_e/D_p=0.6$)

$$t^* = \frac{U_p t}{D_p} \tag{1a}$$

This formation time is equivalent to the dimensionless piston stroke divided by the piston diameter $t^*=L_p/D_p$. A nondimensional circulation can be defined by

$$\Gamma^* = \frac{\Gamma}{U_p D_p} \tag{1b}$$

although other alternatives were suggested [3,13], while Gharib et al. [5] preferred using the dimensional form of the circulation. In a similar way, a nondimensional formation time and circulation, based on the nozzle-exit parameters, can be defined as

$$t_e^* = \frac{U_e t}{D_e} \quad \text{and} \quad \Gamma_e^* = \frac{\Gamma}{U_e D_e} \tag{2}$$

where the spatial average velocity is $U_e=U_p(D_p/D_e)^2$. The relationship between the two formation time definitions is $t_e^*=t^*/(D_e/D_p)^3$. As D_e/D_p decreases, the inflow duration to reach a given t_e^* is shorter. For example, to reach a formation time of $t_e^*=4$ requires a piston stroke of $t^*=L_p/D_p=4$, 2.1, 0.85, 0.25, and 0.03 for a nozzle with $D_e/D_p=1$, 0.8, 0.6, 0.4, and 0.2, respectively.

The Reynolds number, based on nozzle-exit parameters, is Re $=2500$, 1250, 830, 625, and 500 for the nozzles with $D_e/D_p=0.2$, 0.4, 0.6, 0.8, and 1.0, respectively. Consequently, in all the simulations, a laminar flow is assumed, although the case with Re$=2500$ might be transitional [2,20].

2.3 Validation With Experiments. A set of digital particle image velocimetry (DPIV) experiments with a nozzle of $D_e/D_p=0.6$ have been performed for validating the numerical simulations. The experimental setup is described in Ref. [7]. A nearly impulsive velocity program, as recorded in the experiments (with a mean velocity of $U_p\cong 5.7$ cm/s), was imposed in the simulations. The circulation is a major quantity of interest in the present study, and therefore, the measured and calculated evolution of the circulation are compared in Fig. 2. Excellent agreement is obtained.

3 The Flow Inside the Vortex Generator

The efflux of circulation and other motion invariants, and the vortex ring formation are determined by the velocity profile at the exit of the vortex generator, e.g., Refs. [10,12,21]. This emerging

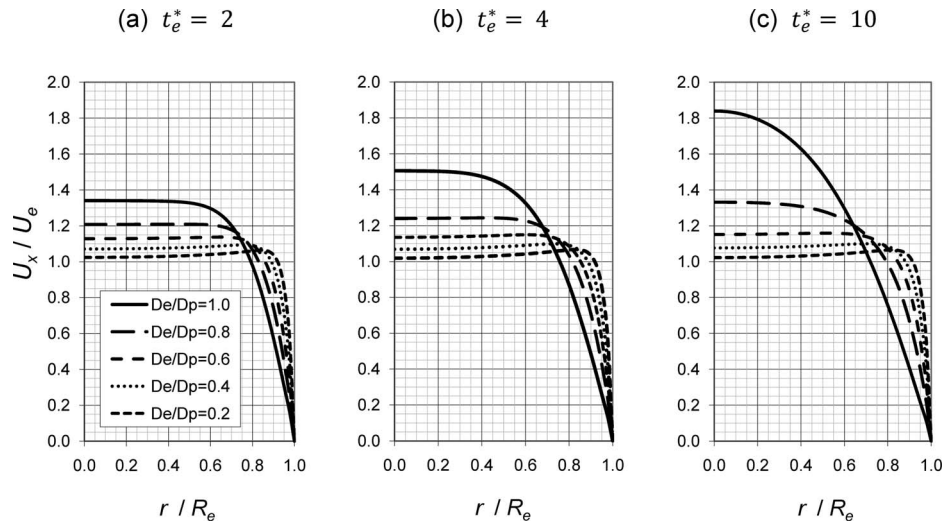

Fig. 3 The evolution of the axial velocity profile at the nozzle exit (velocity program no. 1)

flow is affected by the dynamics of the flow inside the vortex generator. In this section, the characteristics of the nozzle-exit flow are investigated.

In the straight segment of the vortex generator, the flow properties in the initial phase of the flow are similar to that described in Refs. [21,22]. A Stokes layer is created along the straight tube wall with the instantaneous start of the inflow. As the inflow continues, a developing flow in the upstream part is established, and it advances downstream with time. By $t^*=12$, a stationary flow is obtained along the entire straight segment of the tube with an almost parabolic velocity profile at the downstream end. Another observation is that the flow entering the conic cross section is found to be independent of the nozzle geometry.

The converging shape of the nozzle accelerates the mean flow, influencing the boundary layer thickness, and consequently, the efflux of circulation, impulse, and kinetic energy. It also changes the Reynolds number of the emerging flow. The favorable pressure gradient decreases the thickness of the boundary layer. As the exit diameter decreases, the boundary layer thinning is more pronounced, resulting in a more uniform exit velocity profile and a thinner shear layer.

To examine more closely the nozzle-exit flow, Fig. 3 plots the axial velocity profile for formation times of $t_e^*=2$, 4, and 10, and for the different exit diameter nozzles in the case of velocity program no. 1. The first formation time ($t_e^*=2$) is in the roll up phase of the vortex ring, the second ($t_e^*=4$) is approximately equal to the formation number of a straight tube, and in the latter instant ($t_e^*=10$), the leading vortex ring has propagated downstream, far enough to not affect the flow at the nozzle exit (see Fig. 4). The theory of Gharib et al. [5] predicts that the vortex ring properties are determined by the ejection characteristics up to a formation time of $F^*=t_e^*\approx 4$ (for the case of a straight tube vortex generator); this value is also referred to as the formation number [5]. Looking at the nozzle-exit profile reveals that for $D_e/D_p<0.8$, the flow is (i) quasisteady in the core and (ii) a thin Stokes layer exists in an otherwise uniform velocity profile. For $D_e/D_p<0.8$, the axial velocity profile has enough dimensional time to develop into a nearly parabolic profile for $D_e/D_p=1$.

4 Vortex Dynamics and Circulation Evolution

4.1 Vorticity Evolution. The vorticity field for $t_e^*=2$, 4, and 10 is shown in Fig. 4 for all the nozzle cases and for velocity program no. 2, with the inflow stopping at $t_e^*=8$. The vorticity is normalized by U_e/D_e, and the axial and radial coordinates by D_e. This straightforward normalization reveals the similarity in the vorticity distribution for all the nozzle cases. In the formation phase, the more constricted nozzles exhibit a smaller and more concentrated vortex core, originating from the thinner vortex sheet. Significant differences in the vorticity distribution are noticeable only after the formation phase ($t_e^*>4$). The thicker shear layers generated at the lower Reynolds number cases (i.e., larger D_e/D_p) create a thicker core vortex ring, as was also observed by Mohseni et al. [13] for a straight tube vortex generator. The decrease in D_e/D_p has a dual effect regarding viscosity. First, the Reynolds number (based on the exit parameters) increases linearly; for $D_e/D_p=1$, it increases to Re=500, while for $D_e/D_p=0.2$, it increases to Re=2500. Second, as D_e/D_p decreases, the physical time decreases as well for a given t_e^*, and consequently, viscosity has less time to act through vorticity decay and vorticity cancellation. The combined effect of these two factors is a larger vorticity magnitude and thinner core vortex ring as D_e/D_p decreases. At the latest formation time shown ($t_e^*=10$), the vorticity decay and vorticity cancellation have a prominent effect on the vorticity distribution for $D_e/D_p\geq 0.8$. In the case of $D_e/D_p=0.2$, the vorticity accumulated in the tail is susceptible to the Kelvin–Helmholtz instability due to the large Reynolds number of the emerging flow.

4.2 Total Circulation Evolution. Normalization of the total circulation by piston parameters might be appealing since it is common to all the cases considered in the present study. However, the similarity found in the normalized vorticity field, Fig. 4, supports the normalization of the circulation with the nozzle-exit pa-

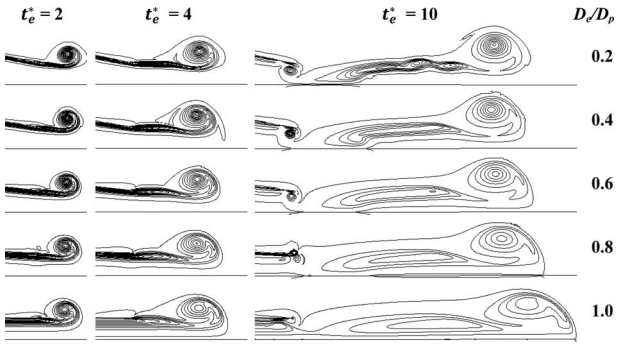

Fig. 4 The scaled vorticity (contour lines between 0 to 20 with an increment of 1) for velocity program no. 2. The spatial coordinates are scaled by D_e.

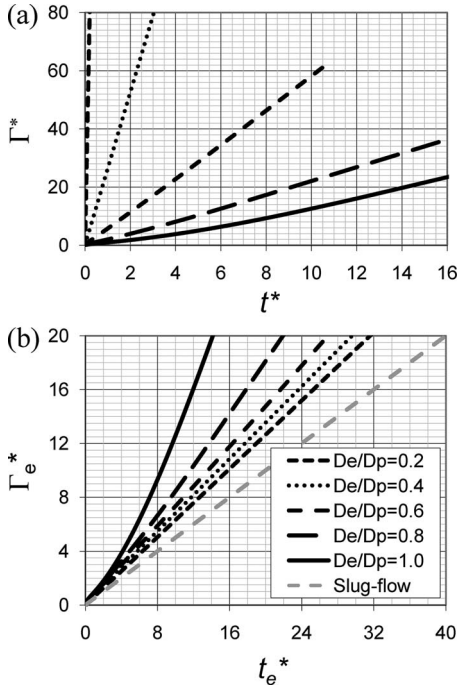

Fig. 5 The evolution of the total circulation, (*a*) normalization by piston parameters, and (*b*) normalization by exit parameters

rameters. To test these normalizations of the circulation, the evolution of the total circulation is depicted in Fig. 5 for the continuous velocity program no. 1. Normalization by the piston or the exit parameters are plotted in Figs. 5(*a*) and 5(*b*), respectively. The total circulation is calculated by integrating the vorticity field in the region outside of the straight tube vortex generator.

The circulation Γ^* (that is also proportional to the dimensional circulation) can be significantly increased by decreasing the exit diameter of the nozzle, Fig. 5(*a*). The dependence of Γ_e^* on D_e/D_p is smaller. In the latter normalization, the smallest D_e/D_p exhibits the lowest normalized circulation for a given t_e^*. The circulation, as predicted by the slug model, is also plotted in Fig. 5(*b*). In all the nozzle cases, the circulation is larger than the slug model prediction. The deviation decreases as D_e decreases due to the more uniform exit velocity profile (Fig. 3) that conforms with the slug model approximation.

None of these normalizations could collapse the evolution of the total circulation of all the nozzle cases into a single line, although the same velocity program of the piston is employed. In an attempt to alleviate this, an alternative normalization of the circulation and formation time is suggested hereof. It will also allow separating between two contributions to the ejected circulation, a slug-type one-dimensional flow contribution, and an inherently two-dimensional flow contribution.

4.3 The Two-Dimensional Contribution to Circulation. The circulation flux ejected out of the nozzle (neglecting diffusive fluxes) can be decomposed [1,19] into

$$\frac{d\Gamma}{dt} = \int_0^{D_e/2} u\omega dr = \frac{1}{2}U_{\mathrm{cl}}^2 + \int_0^{D_e/2} u\frac{\partial v}{\partial x}dr \tag{3}$$

where u and v are the axial (x) and radial (r) velocity components, respectively, w is the azimuthal vorticity, and U_{cl} is the exit centerline velocity. The time integration of this circulation is identical to the total circulation (except a small deviation during the early formation of the vortex due to the generation of vorticity at the outer lip of the nozzle). This form suggests the following normalization:

$$t^{**} = \frac{\tilde{U}t}{D_e}$$
$$\Gamma^{**} = \frac{\Gamma}{\tilde{U}D_e} \tag{4}$$

where the velocity scale $\tilde{U} = \sqrt{\bar{U}_{\mathrm{cl}}^2}$ is the running mean velocity $\bar{U}_{\mathrm{cl}}^2 = \frac{1}{t}\int_0^t U_{\mathrm{cl}}^2 d\tau$. The integration of Eq. (3) using the normalization of Eq. (4) leads to

$$\Gamma^{**} = \frac{t^{**}}{2} + \frac{1}{\tilde{U}D_e}\int_0^t \int_0^{D_e/2} u\frac{\partial v}{\partial x}drd\tau \tag{5}$$

The first term is the contribution related to the one-dimensional flow, while the second term originates from the inherently two-dimensional flow at the exit.

In the generalized slug model, the two-dimensional contribution is neglected, resulting in $\Gamma^{**} = t^{**}/2$, or in dimensional form $\Gamma = (1/2)\bar{U}_{\mathrm{cl}}^2 t$, i.e., the circulation ejected out of the vortex generator depends on the centerline exit velocity rather than the mean velocity that is used in the original slug model. The generalized slug model extends the original slug model into cases with a nonuniform axial velocity profile, while keeping the assumption of a one-dimensional flow at the exit, see for example Ref. [19]. In many previous studies, short ejection time and high Reynolds number cases have been considered, leading to flows with thin boundary layers with the mean velocity almost identical to the centerline velocity. Shusser et al. [21] introduced a first-order approximation that corrected the centerline velocity as a result of the evolution of a thin Stokes layer, leading to an improved estimation of the circulation generation for intermediate ejection times. In the cases of long ejection times and/or low Reynolds number flows, as in the present study, it is necessary to employ the generalized slug model to account for the enhanced circulation generation, due to the exit parabolic-like velocity profile.

The second contribution to the circulation (Eq. (5)) is significant only when the exit flow is two-dimensional, i.e., when the integral of $u(\partial v/\partial x)$ is significant. Most existing studies ignore this inherently two-dimensional contribution. Didden [1] and Krueger [19] realized the importance of the two-dimensional contribution to circulation generation in the case of straight tube vortex generators. Krueger [19] showed that for nearly impulsive velocity programs, a noticeable two-dimensional flow is formed at a very short time during the initiation of the flow. This results in a small constant circulation offset ($\Gamma^* \approx 1/\pi$) to the (classical) slug model. Krueger [19] related this offset to the overpressure that develops during the initial phases of the flow.

In the present case of conic nozzles, a significant two-dimensional contribution is expected *throughout* the ejection phase due to the shape of the exit nozzle that enforces a two-dimensional flow. Figure 6 plots Γ^{**} versus t^{**} for the (continuous) velocity program no. 1. Less dependence of Γ^{**} on D_e/D_p is obtained than in the previous normalizations (Fig. 5), indicating the relatively large one-dimensional contribution. The slope, however, does depend on D_e/D_p. The smaller D_e/D_p is, the larger the slope is and the larger is the deviation of Γ^{**} from the generalized slug model, i.e., the two-dimensional contribution is more significant. To assess the relative two-dimensional contribution to the circulation flux throughout the continuous ejection, $d\Gamma^{**}/dt^{**}$ versus t^{**} is plotted in Fig. 7(*a*). Any deviation of $d\Gamma^{**}/dt^{**}$ from 1/2 originates from two-dimensional effects at the exit. Moreover, the magnitude of the difference is proportional to the relative two-dimensional contribution to the total circulation generation. It should be noted, however, that the *magnitude* itself of the one-dimensional contribution cannot be evaluated from the normalized Γ^{**} (since $\Gamma^{**} \equiv 1/2$ by definition).

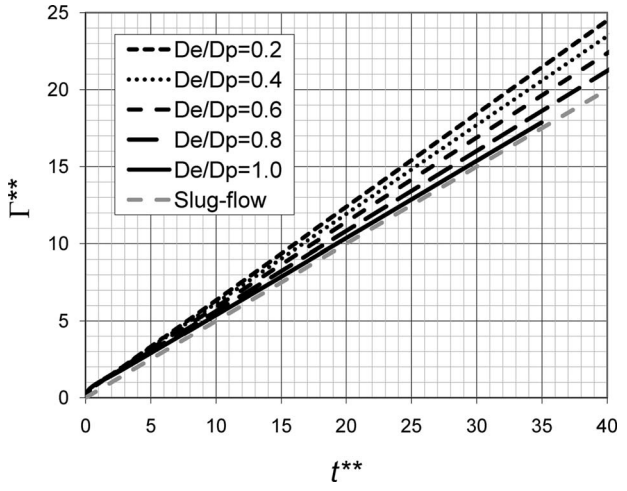

Fig. 6 The evolution of the double-star normalized circulation

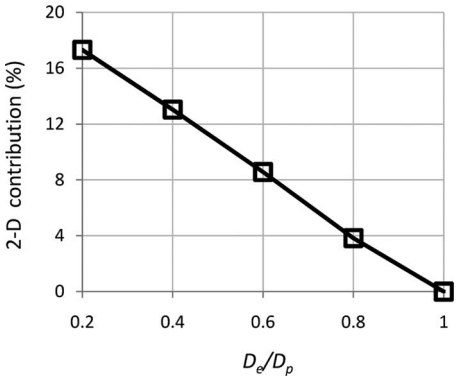

Fig. 8 The asymptotic two-dimensional contribution to the total circulation generation (%)

With the impulsive initiation of the flow, a very large $d\Gamma^{**}/dt^{**}$ is obtained, in agreement with the analysis of Krueger [19]. These effects are significant up to $t^{**} \approx 1/2$, i.e., in the initial forming phase of the vortex ring. In contrast to the findings of Krueger [19] for a straight tube, the two-dimensional effects do not vanish after the initiation of the flow. Rather, $d\Gamma^{**}/dt^{**}$ approaches a constant asymptotic value greater than 1/2 in the converging nozzle cases. Figure 8 plots the asymptotic ratio of the two-dimensional contribution to the total circulation. It increases linearly with the decrease in D_e/D_p up to a value of 17%.

Krueger [19] used the centerline exit pressure p_{cl} to evaluate the 2D contribution to the circulation instead of the "double-star" normalization employed in the present study. He also pointed out the equivalence of p_{cl}/ρ (ρ is the density) to the two-dimensional contribution $\int_0^{D_e/2} u(\partial v/\partial x)dr$. Indeed, plotting the calculated $p_{cl}/\rho U_e^2$ versus t_e^*, Fig. 7(*b*), yields a very similar plot to Fig. 7(*a*). The persisting two-dimensional contribution of the constricted conic nozzles can be also noticed in the nonvanishing asymptotic value of p_{cl} for $D_e/D_p < 1$. One can notice for $D_e/D_p > 0.6$ that for a brief period in the formation phase ($t_e^* \cong 1$), the 2D effects contribute a *negative* circulation flux ($d\Gamma^{**}/dt^{**} < 1/2$ in Fig. 7(*a*), and $p_{cl}/\rho U_e^2 < 0$ in Fig. 7(*b*)). For larger exit diameter cases, the negative two-dimensional contribution cancels out a portion of the circulation added in the flow initiation phase. This occurs when the vortex ring is developed enough to induce a significant negative radial velocity at the exit, reversing the sign of $\partial v/\partial x$. With the translation of the vortex ring farther downstream, the sign of $\partial v/\partial x$ changes back to positive (in the case of $D_e/D_p < 1$).

5 Vortex Ring Properties

The evolutions of total and vortex ring circulations (both normalized by the exit parameters) are shown in Fig. 9 for velocity program no. 2 (the inflow is stopped at $t_e^* = 8$). The maximal vortex ring circulation is given in Table 1 for the various D_e/D_p cases. For $D_e/D_p \geq 0.8$, the enhanced circulation efflux increases the normalized vortex ring circulation as well. For the straight tube case ($D_e/D_p = 1$), it is $\Gamma_{e,V}^* = 3.8$, significantly larger than the vortex circulation of $\Gamma_{e,V}^* \approx 2.7$ found by Rosenfeld et al. [10] for a uniform exit velocity profile. In the case of an imposed *parabolic* exit velocity profile, they have obtained a larger vortex circulation of $\Gamma_{e,V}^* = 3.5$, close to the value calculated in the present study for the straight tube. The relatively low Reynolds number flow in the present straight tube case (Re=500) results in a parabolic-like exit velocity profile (Fig. 3), and hence, the increase in the vortex circulation. The augmented vortex circulation is accomplished by an axis-touching vortex ring that resembles a Hill's spherical vortex, Fig. 4. For smaller exit diameter cases ($D_e/D_p < 0.6$), the vortex circulation reduces to $\Gamma_{e,V}^* = 2.7$, identical to the values obtained for a uniform exit velocity profile [10,12].

To further study the formation process, the evolution of the normalized energy ejected out of the nozzle, as well as the normalized energy of the vortex ring, are plotted in Fig. 10. Following Gharib et al. [5], the normalized energy is defined as $e = E/\sqrt{I\Gamma^3}$, where E is the kinetic energy, and I is the impulse. The normalized vortex ring energy is very useful in studying the dy-

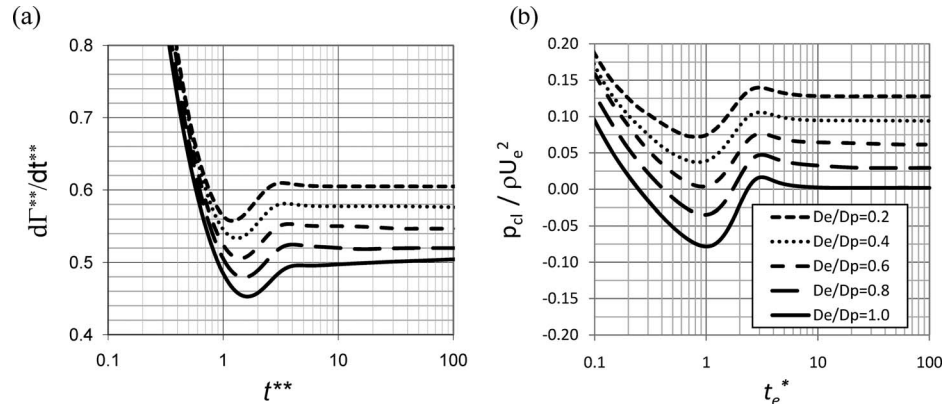

Fig. 7 The evolution of (*a*) the normalized circulation flux versus the formation time t^{**}, and (*b*) the centerline exit pressure versus t_e^*

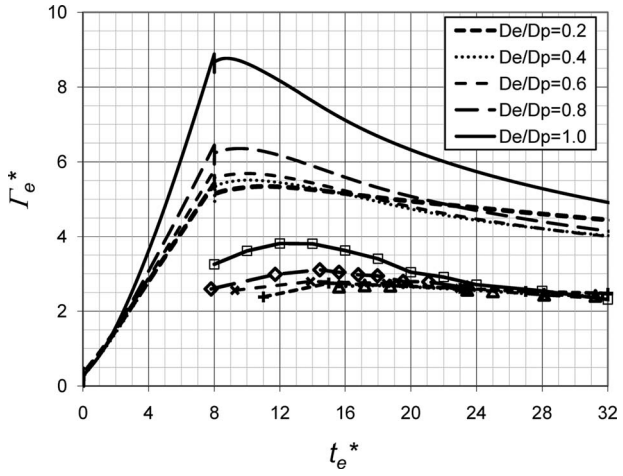

Fig. 9 The evolutions of the total (lines) and vortex ring (lines with symbols) circulations

namics of vortex rings as it invokes the three motion invariants being delivered by the vortex generator. The dependence of the maximal vortex ring energy on the nozzle-exit diameter is also given in Table 1. Unlike the normalized circulation, the normalized kinetic energy is larger for the more constricted nozzles, resulting in more energetic vortex rings for a given circulation and impulse. The decrease of e with the increase in D_e/D_p is related to the shape (vorticity distribution) of the vortex ring, as can be seen in Fig. 4. With the increase in D_e/D_p and the associated decrease in the Reynolds number, the vortex ring transforms from a thin core concentrated vortex ring into a thick core axis-touching vortex that resembles the Hill's spherical vortex. Gharib et al. [5] showed that for thin core vortex rings, $e \approx 0.33$ decreases to a value of $e \approx 0.16$ for the Hill vortex. In the present case, the largest vortex energy of $e=0.27$ is found for $D_e/D_p=0.2$, while the smallest is $e=0.21$ for $D_e/D_p=1$. The decrease in the vortex energy with the increase in the vortex circulation was also found by Mohseni et al. [13] for a straight vortex generator. Zhao et al. [12] calculated a vortex energy of $e=0.31-0.34$ for a set of imposed hyperbolic tangent exit axial velocity profiles with thin boundary layers. However, when Zhao et al. [12] imposed a parabolic exit velocity profile, the calculated vortex energy dropped to $e=0.195$. Obviously, developed velocity profiles (with thick shear layers) reduce the normalized energy of the vortex ring.

Table 1 The dependence of the vortex ring parameters on the exit diameter

D_e/D_p	$\Gamma^*_{e,V}$	F^*	e
0.2	2.73	4.1	0.27
0.4	2.69	3.9	0.24
0.6	2.79	3.8	0.22
0.8	3.10	3.9	0.22
1.0	3.80	4.1	0.21

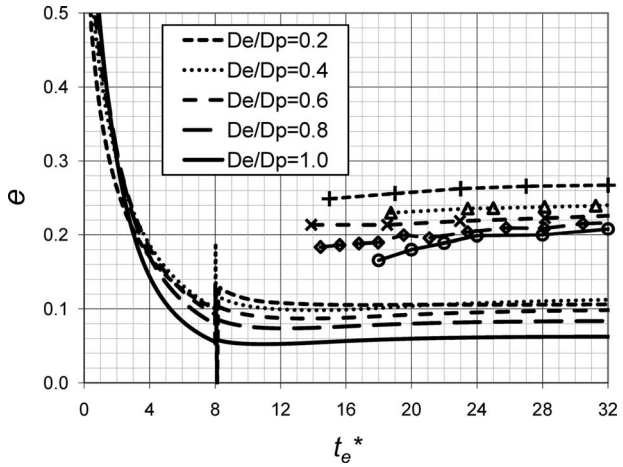

Fig. 10 The evolutions of the total (lines) and vortex ring (lines with symbols) normalized energies

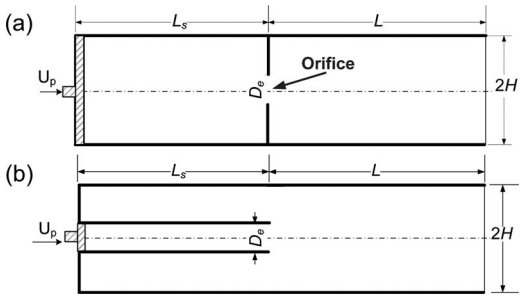

Fig. 11 Geometry of the limiting cases (*a*) orifice and (*b*) straight tube vortex generators (D_e=1.5 cm, H=10 cm, L_s=45.1 cm, and L=80 cm)

Despite the dependence of the circulation efflux and vortex ring circulation on the conic nozzle-exit diameter, the formation number, as defined by Gharib et al. [5], yields an almost constant value of $F^*=3.85\pm0.25$, Table 1, well within the range found in previous experimental and computational studies of straight tube vortex generators, see for example Refs. [5,10,13]. The invariance of the formation number with the exit diameter is a consequence of the finding that the increase in the ejected circulation, as D_e/D_p increases, is accompanied by an increase in the vortex ring circulation as well.

6 Effect of the Nozzle Length

So far, only one factor of the conic nozzle has been considered: the exit diameter, while the length of the nozzle was kept constant. The shortening of the nozzle is expanded to increase the two-dimensional contribution. A limiting case is a zero-length nozzle—i.e., an orifice, see Fig. 11(*a*). Such a case with an orifice diameter of $D_e=1.5$ cm, equal to the exit diameter of the conic nozzle $D_e/D_p=0.6$, has also been simulated. It should be noticed that in most previous vortex ring formation studies that refer to an orifice case, e.g., Refs. [5,10], the geometry is different. It consists of a flat plate, flushed with the exit of a straight tube with a small diameter (D_p rather than $2H$, as in the present case). The most significant difference is that in the latter case, the flow at the exit is mostly parallel to the wall of the tube, while in the present case, there is a large radial component of the flow, upstream of the orifice, that leads to a large axial gradient of the radial velocity component, and consequently, to a significant two-dimensional contribution to the circulation production.

Yet another limiting case that has been simulated is that of a straight tube vortex generator with a constant diameter equal to the diameter of the orifice ($D_e=D_p=1.5$ cm), Fig. 11(*b*). The inflow rate identical to previous conic nozzle cases is employed in these two additional simulations as well, maintaining the same exit Reynolds number as of the conic nozzle with $D_e/D_p=0.6$ (Re=830).

The exit centerline velocity determines the magnitude of the one-dimensional contribution, Eq. (3). The evolution of the exit centerline velocity for these three identical exit diameter cases is shown in Fig. 12. In all the cases, the initiation of the flow ($t_e^*<1$) is accompanied by an overshoot of the exit velocity profile near the walls, leading to a centerline velocity lower than the

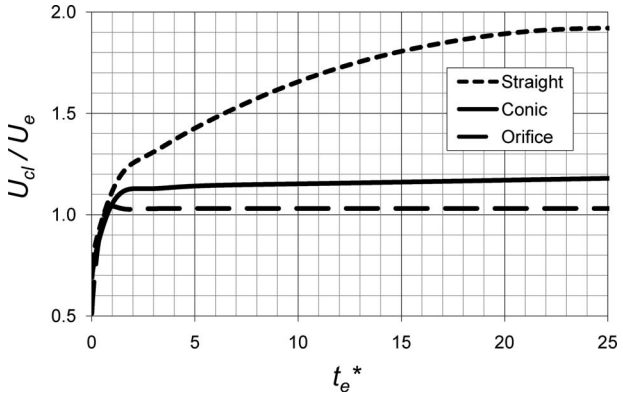

Fig. 12 The evolution of the exit centerline velocity for the cases with an equal exit diameter (D_e=1.5 cm)

mean exit velocity. Afterwards, the exit velocity profile of the orifice case is almost uniform and steady ($U_{cl}/U_e \approx 1.03$). The conic nozzle has a less uniform axial velocity but only by a small amount ($U_{cl}/U_e \approx 1.15$). However, it does evolve slowly in time. In the straight tube case, the velocity profile develops into a nearly parabolic flow ($U_{cl}/U_e \approx 1.92$) by $t_e^*=20$.

The evolutions of Γ_e^* and $d\Gamma^{**}/dt^{**}$ are plotted in Fig. 13. The circulation generated by the conic nozzle and straight tube cases are almost identical during the starting phase of the flow ($t_e^*<3$), when the exit velocity profile is almost uniform. Only later on ($t_e^*>4$), with the increase in the centerline velocity, the straight tube generates a larger circulation (attributed to the one-dimensional contribution). The growth of the centerline velocity increases the slope $d\Gamma_e^*/dt_e^*$ as well, until $t_e^* \sim 20$, when an almost fully developed flow is attained. Subsequently, the exit flow becomes stationary, and the circulation efflux is also steady.

The two-dimensional contribution in the orifice case is larger than in the other two cases (it contributes as much as 44% of the total contribution), generating a larger overall circulation efflux up to $t_e^*=8$. Afterwards, the continuous increase in the centerline exit velocity of the straight tube case generates a significantly larger circulation than the orifice case. Yet, the larger two-dimensional contribution of the orifice leads to the generation of a larger circulation than in the conic nozzle case.

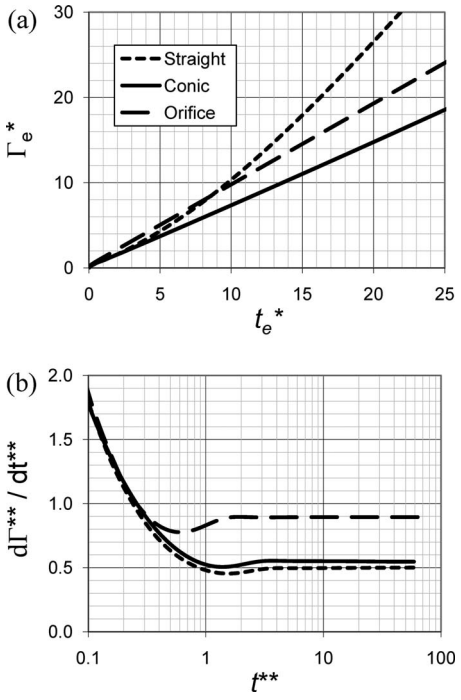

Fig. 13 Evolution of the (*a*) circulation and (*b*) circulation flux for the cases with an equal exit diameter (D_e=1.5 cm)

Table 2 Vortex ring parameters for three cases with identical exit diameter (D_e=1.5 cm)

	$\Gamma_{e,V}^*$	F^*	e
Straight tube	3.99	4.2	0.18
Conic nozzle	2.79	3.8	0.22
Orifice	3.83	3.7	0.24

The vortex circulation and normalized energy, as well as the formation number of these cases, are summarized in Table 2. The straight tube and orifice cases generate significantly larger circulation vortices: $\Gamma_{e,V}^*=3.99$ and 3.83, respectively, as a result of the larger circulation efflux during the vortex formation phase. The circulation production is larger either due to a larger centerline velocity (i.e., one-dimensional contribution) in the straight tube case, or due to the two-dimensional contribution in the orifice case. In the conic nozzle case that is characterized by an almost uniform exit velocity profile and relatively small (~9%) two-dimensional contribution, the vortex circulation is in the range reported previously for straight tubes with uniform exit velocity ($\Gamma_{e,V}^* \cong 2.8$).

The formation number is within the common range, in agreement with the previous findings of the present study. The almost uniform exit velocity profile of the orifice case yields the largest vortex energy (e=0.24), while the straight tube with the nonuniform exit velocity profile generates the least energetic vortex ring e=0.18. The lower energy of the vortex ring is consistent with the higher formation number since pinch-off occurs later (the feeding vortex sheet is disconnected only when the vortex ring energy exceeds that of the feeding flow [5]).

7 Conclusions

The present study presented evidences on the importance of the vortex generator geometry, and in particular, the exit configuration on the generation of circulation and on the vortex ring properties in the case of long ejection times. Conic nozzles allow flow manipulation by increasing the exit mean velocity and the Reynolds number, and by enforcing a two-dimensional flow at the exit. While the one-dimensional contribution is proportional to the square of the centerline exit velocity, and therefore, to approximately the fourth power of D_p/D_e (keeping the same volumetric flow rate), the two-dimensional contribution is found to be linear with D_p/D_e.

The control of the circulation ejection (as well as other motion invariants) is a target of any vortex ring optimization procedure. The one-dimensional contribution to the circulation is determined by the magnitude of the exit centerline velocity. It is a function of time and of the geometry of the vortex generator. Consequently, the control of the one-dimensional contribution is limited and indirect in nature. A more straightforward control can be obtained by manipulating the *two-dimensional* contribution through shaped nozzles, such as conic nozzles. The two-dimensional contribution persists the *entire* duration of the ejection, affecting the circulation rate as well. The double-star normalization has the advantage of allowing a quantitative assessment of the two-dimensional contribution *relative* to the one-dimensional contribution, while the alternate form of Krueger [19] cannot provide such a quantitative comparison. It has been found that the two-dimensional contribution to the circulation increases as the cone opening angle increases (i.e., the exit diameter decreases), and consequently, the

circulation generation increases as well. In the limiting case of an orifice (with an opening angle of 90 deg), the two-dimensional contribution is as large as 44% of the total circulation production. In the conic cases considered in the present study, the maximal two-dimensional contribution (17%) is obtained for the smallest exit diameter case ($D_e/D_p=0.2$).

The increase in the circulation generation rate is accompanied by an increase in the vortex ring circulation as well, keeping the formation number almost constant, $F^* \approx 4$. Thus, conic nozzles affect the magnitude of circulation or energy but not the strategy for obtaining optimal values. Thus, optimization of thrust or other quantities should employ techniques similar to previous studies of straight tube vortex generators, e.g., Refs. [6,14].

Nomenclature

D = diameter
E = kinetic energy (g cm/s^2)
e = normalized kinetic energy
F^* = formation number
H = distance of the outer boundary (from the axis) (cm)
I = impulse (g cm/s)
L = length of the computational domain (from the nozzle exit) (cm)
L_p = piston stroke (cm)
L_n = length of the conic segment of the tube (cm)
L_s = length of the straight segment of the tube (cm)
p = pressure (dyn/cm^2)
Re = Reynolds number
t = time (s)
t_e^* = formation time based on exit parameters (Eq. (2))
t^* = formation time based on piston parameters (Eq. (1))
t^{**} = double-star formation time (Eq. (4))
u, v = the axial and radial velocity components (cm/s)
$\tilde{U}$ = velocity scale $\tilde{U}=\sqrt{\bar{U}_{\mathrm{cl}}^2}$, where $\bar{U}_{\mathrm{cl}}^2=1/t\int_0^t U_{\mathrm{cl}}^2 d\tau$
U = nozzle exit axial velocity (cm/s)
x, r = axial and radial coordinates (cm)

Greek Symbols

ρ = density (g/cm^3)
ω = azimuthal vorticity (1/s)
Γ = circulation ejected out of the tube (cm^2/s)
Γ^* = normalized circulation based on piston parameters (Eq. (1))
Γ_e^* = normalized circulation based on exit parameters (Eq. (2))
Γ^{**} = double-star normalized circulation (Eq. (4))

Subscripts

cl = nozzle exit centerline
e = nozzle exit
p = piston

References

[1] Didden, N., 1979, "Formation of Vortex Rings—Rolling-Up and Production of Circulation," Z. Angew. Math. Phys., **30**(1), pp. 101–116.
[2] Glezer, A., 1988, "The Formation of Vortex Rings," Phys. Fluids, **31**(12), pp. 3532–3542.
[3] Glezer, A., and Coles, D., 1990, "An Experimental-Study of a Turbulent Vortex Ring," J. Fluid Mech., **211**, pp. 243–283.
[4] Shariff, K., and Leonard, A., 1992, "Vortex Rings," Annu. Rev. Fluid Mech., **24**, pp. 235–279.
[5] Gharib, M., Rambod, E., and Shariff, K., 1998, "A Universal Time Scale for Vortex Ring Formation," J. Fluid Mech., **360**, pp. 121–140.
[6] Krueger, P. S., and Gharib, M., 2003, "The Significance of Vortex Ring Formation to the Impulse and Thrust of a Starting Jet," Phys. Fluids, **15**(5), pp. 1271–1281.
[7] Dabiri, J. O., and Gharib, M., 2004, "Fluid Entrainment by Isolated Vortex Rings," J. Fluid Mech., **511**, pp. 311–331.
[8] Krueger, P. S., Dabiri, J. O., and Gharib, M., 2006, "The Formation Number of Vortex Rings Formed in Uniform Background Co-Flow," J. Fluid Mech., **556**, pp. 147–166.
[9] Pullin, D. I., 1979, "Vortex Ring Formation at Tube and Orifice Openings," Phys. Fluids, **22**(3), pp. 401–403.
[10] Rosenfeld, M., Rambod, E., and Gharib, M., 1998, "Circulation and Formation Number of Laminar Vortex Rings," J. Fluid Mech., **376**, pp. 297–318.
[11] Mohseni, K., and Gharib, M., 1998, "A Model for Universal Time Scale of Vortex Ring Formation," Phys. Fluids, **10**(10), pp. 2436–2438.
[12] Zhao, W., Frankel, S. H., and Mongeau, L. G., 2000, "Effects of Trailing Jet Instability on Vortex Ring Formation," Phys. Fluids, **12**(3), pp. 589–596.
[13] Mohseni, K., Ran, H. Y., and Colonius, T., 2001, "Numerical Experiments on Vortex Ring Formation," J. Fluid Mech., **430**, pp. 267–282.
[14] Linden, P. F., and Turner, J. S., 2001, "The Formation of "Optimal" Vortex Rings, and the Efficiency of Propulsion Devices," J. Fluid Mech., **427**, pp. 61–72.
[15] Gharib, M., Rambod, E., Kheradvar, A., Sahn, D. J., and Dabiri, J. O., 2006, "Optimal Vortex Formation as an Index of Cardiac Health," Proc. Natl. Acad. Sci. U.S.A., **103**(16), pp. 6305–6308.
[16] Dabiri, J. O., Colin, S. P., and Costello, J. H., 2006, "Fast-Swimming Hydromedusae Exploit Velar Kinematics to Form an Optimal Vortex Wake," J. Exp. Biol., **209**(11), pp. 2025–2033.
[17] Allen, J. J., and Naitoh, T., 2005, "Experimental Study of the Production of Vortex Rings Using a Variable Diameter Orifice," Phys. Fluids, **17**, p. 061701.
[18] Dabiri, J. O., and Gharib, M., 2005, "Starting Flow Through Nozzles With Temporally Variable Exit Diameter," J. Fluid Mech., **538**, pp. 111–136.
[19] Krueger, P. S., 2005, "An Over-Pressure Correction to the Slug Model for Vortex Ring Circulation," J. Fluid Mech., **545**, pp. 427–443.
[20] Naitoh, T., Fukuda, N., Gotoh, T., Yamada, H., and Nakajima, K., 2002, "Experimental Study of Axial Flow in a Vortex Ring," Phys. Fluids, **14**(1), pp. 143–149.
[21] Shusser, M., Gharib, M., Rosenfeld, M., and Mohseni, K., 2002, "On the Effect of Pipe Boundary Layer Growth on the Formation of a Laminar Vortex Ring Generated by a Piston/Cylinder Arrangement," Theor. Comput. Fluid Dyn., **15**(5), pp. 303–316.
[22] Heeg, R. S., and Riley, N., 1997, "Simulations of the Formation of an Axisymmetric Vortex Ring," J. Fluid Mech., **339**, pp. 199–211.